Alkali Metal Bonding Energy and Activation Energy for dc Conductivity in Porous and Glassy Solid Oxides

F. Henn,*,† S. Devautour-Vinot,† J. C. Giuntini,† and G. Maurin‡

Laboratoire de Physicochimie de la Matière Condensée, UMR 5617 CNRS, Université Montpellier II, Place Eugene Bataillon, 34095 Montpellier Cedex 5, France, and Laboratoire MADIREL, UMR 6121 CNRS, Université de Provence, Centre de Saint-Jérôme, 13397 Marseille Cedex 20, France

Received: January 14, 2004; In Final Form: June 30, 2004

A model for the alkali metal bonding energy in some solid oxides based on a simplified approach of the electronegativity equalization method is proposed. From this model, no intensive numerical calculation is required. The bonding energy can be written as a linear combination of three independent energy contributions, namely, an electrostatic term, a covalent term, and a polarization term, that are expressed as a function of the alkali metal cation radius. The model is then used to fit the evolution of the activation energy for the dc conductivity with the various alkali metal cations in the following test cases: a clay mineral (montmorillonite), two zeolites (faujasites Fau-X and Fau-Y), three glassy oxides (a silicate with two alkali contents and a triborate). Two typical behaviors can be distinguished: (i) the considered solid oxide is either porous or supposed to have enough free volume for the displacement of the cation, in which case the model can be applied, and (ii) the compactness of the structure is such that the analytical expression for activation energy for the dc conductivity contains an additional term, in which case the model cannot be directly used. However, if this additional energy is known, then it is possible to estimate the alkali metal bonding energy and to properly reproduce it from the model. Finally, it is shown that, when the model is applicable, it yields relevant information about both the nature of the alkali metal bond and the microscopic mechanism involved in the dc conductivity. This information is in nice agreement with what we know about the structure of the considered solid oxides.

I. Introduction

Despite the critical role played by alkali metal cations in many solid oxides (materials for battery application, adsorption/catalytic/cationic exchange properties in nanoporous aluminosilicates, exchange and transport properties in membranes, etc.) and the resulting extensive experimental and theoretical work carried out on these solids, there is still no widely accepted theory to explain the evolution of the activation energy for dc conductivity, $\Delta E_{\sigma_{dc}}$, or for the alkali metal−oxide bonding energy, ΔE_{bond}, when a given alkali metal cation is substituted by another one.

First, it must be recalled that $\Delta E_{\sigma_{dc}}$ can be formally seen as the sum of two contributions

$$\Delta E_{\sigma_{dc}} = \Delta E_{bond} + \Delta E_{\mu} \quad (1)$$

where ΔE_{bond} is the cation−oxide bonding energy, i.e., the energy necessary for extracting a given cation from its potential minimum, and ΔE_{μ} is the energy related to the cation migration over a long distance.

The lack of a universal explanation could then arise from this duality. First, it is likely that both ΔE_{bond} and ΔE_{μ} vary independently and differently from oxide to oxide, depending on both the chemical species involved and the structure[1] of the material. Second, the respective evolutions of ΔE_{bond} and ΔE_{μ} cannot be readily determined from the experimental values of $\Delta E_{\sigma_{dc}}$ because they cannot always be separated.

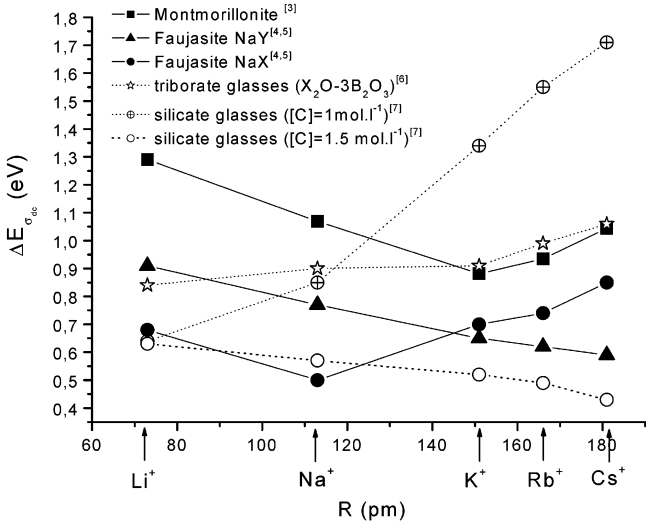

Figure 1. Activation energy for dc conductivity in various porous and glassy oxides. Symbols are the experimental data (see figure legend for the references). Full lines are just to guide the eyes. [C] is the concentration of alkali metal cation.

The complexity of this problem can be illustrated as in Figure 1 where we report the evolution of $\Delta E_{\sigma_{dc}}$ for a variety of alkali metal cations in various porous and glassy test-case solid oxides. In principle, only glassy solid oxides and oxides that are porous and have exchangeable alkali metal cations can be studied because their structures are not strongly dependent on the nature

* To whom correspondence should be addressed. E-mail: fegh@lpmc.univ-montp2.fr.
† Université Montpellier II.
‡ Université de Provence.

10.1021/jp049802x CCC: $27.50
Published on Web 08/20/2004

of the cation. A direct comparison can then be drawn from the analysis of the whole alkali metal series.[2]

It is clear from Figure 1 that $\Delta E_{\sigma_{dc}}$ exhibits no universal behavior.[3−7] In some cases, this activation energy increases continuously from Li^+ to Cs^+, whereas in some others, it decreases. Evolutions going through a minimum are also observed.

An original model proposed many years ago by Anderson and Stuart (AS model) for glassy silicates[8] assumed that, in addition to the energy ascribed to the electrostatic interaction that binds the alkali metal cation to the solid oxide framework, an energy term associated with deformations, i.e., strain induced by cation migration from site to site, plays a key role. In the AS model, the energy involved in the deformation of the glassy framework is seen as the energy for the cation migration ΔE_μ, and the bonding energy ΔE_{bond} is restricted to the electrostatic term. With this model, eq 1 is obeyed providing ΔE_{bond} equals an electrostatic term, ΔE_{elec}, that is an inverse function of the cation radius R_C and ΔE_μ is a parabolic function of R_C.

This model has proved to be valid in many amorphous or crystallized oxides, and it is still applied.[9,10] However, it fails to explain complex behaviors such as those depicted in Figure 1. As qualitatively suggested by Kalogeras et al.[5] for zeolites, these behaviors could be partly due to the covalent character of the alkali−oxide bond, i.e., the possible electronic charge transfer between the alkali metal cation and the oxide framework, which is a nonnegligible factor when considering the evolution of $\Delta E_{\sigma_{dc}}$. This explanation is confirmed by other work[11] where it has been pointed out that the activation energies for dc conductivity in various superionic conductors (oxides and nonoxides) could be scaled from the average value of the electronegativity. It has also recently been demonstrated from computational chemistry[12] on a simple crystallized ionic solid, CuI, that the degree of ionicity of the Cu−I bond, and hence the covalent character of the Cu−I bond, could strongly vary depending on the cation confinement in the tetrahedral or octahedral crystallographic sites. This covalent aspect of the alkali−oxide bond is clearly not taken into account for in the AS model.

Likewise, the cation polarization is not considered. If cation deformation, i.e., polarization, can be supposed to have a limited impact on $\Delta E_{\sigma_{dc}}$ in regard to the framework deformation of compact glassy or crystallized structures, this might not be the case for nanoporous oxides. In the latter, nanoscale voids such as channels, cages, or interlayer spaces offer preferential diffusion paths, and no significant framework deformation is required for the cation displacement. The same feature can be assigned to some glassy or structurally loose oxides in which structural heterogeneity[13,14] can induce favored diffusion paths associated with negligible framework deformation. Superseding the AS model, S. R. Elliott[15] proposed a model in which the polarization is included within the interaction potential. Although this model is more sophisticated and more realistic than the AS model, it cannot reproduce all of the experimental trends reported in Figure 1.

The preliminary confrontation between the experimental data reported in Figure 1 and the existing models indicates that the alkali metal−oxide bond is likely to be more complex than a simple ionic bond and that a more elaborate representation of this bond is needed to explain the experimental behavior. Our aim is therefore to derive such a model that takes into account, beyond the electrostatic energy, two additional energies, namely, the covalent and polarization energies.

In this article, we consider a model that was recently developed by some of us[16] to account for the polarization effects involved in the displacement of alkali metal cations trapped in zeolites. Then, we show how, after further simplifications, it can be extended to reproduce the evolution of ΔE_{bond} with both the various alkali metal cations and solid oxides. The model is based on a simplified approach of the electronegativity equalization method.[17,18] Within this model, the bonding energy, ΔE_{bond}, is defined as a linear combination of three independent energy contributions: an electrostatic term, a covalent term, and a polarization term, each of which is expressed as a function of R_C, the cationic radius.

Then, this model is applied to the test-case oxides reported in Figure 1, and a fit of the experimental results of $\Delta E_{\sigma_{dc}}$ is obtained. It is pointed out that, in certain cases, the model for ΔE_{bond} reproduces well the experimental behavior of $\Delta E_{\sigma_{dc}}$, i.e., $\Delta E_{\sigma_{dc}} \approx \Delta E_{bond}$ and, as a consequence, ΔE_μ can be neglected. Hence, it allows us to qualitatively estimate the respective weights of the electrostatic, covalent, and polarization energy terms involved in ΔE_{bond}. In the other cases, when the model fails to fit the experimental evolution of $\Delta E_{\sigma_{dc}}$, it is shown that the model reproduces the value of ΔE_{bond} whenever it is measurable. This clearly demonstrates the validity of the model for ΔE_{bond} when this energy can be determined or for $\Delta E_{\sigma_{dc}}$ when the mobility term ΔE_μ can be neglected.

II. The Model

The model proposed in this paper is based on the density functional theory of chemical reactivity[19,20] and on the electronegativity equalization method (EEM).[17,18] It aims to yield a qualitative explanation for the experimental evolution of ΔE_{bond} in some oxides and hence to quantitatively determine the relative weights of the electrostatic, covalent, and polarization contributions to the energy of the alkali metal−oxide bond. Strictly speaking, the exact determination of these contributions could be directly achieved using first-principles calculations. However, these simulations are hampered on solid oxides as complex and as large as clay minerals, zeolites, and glassy oxides as the computational work they would require is too intensive. Consequently, the purpose of this work is to propose crude but realistic simplifications that aim to build a convenient method for fitting the experimental data and for acquiring a deeper knowledge of the nature of alkali metal−oxide bonds in these solids.

First, we start from the fact that the energy of the electron cloud of an isolated species can always be related to its electron population N. The energy characteristic of a given population N can then be obtained from a second-order Taylor expansion, near a reference state E_0 characterized by N_0 electrons

$$E(\Delta N) = E_0 + \frac{\partial E}{\partial N}\Delta N + \frac{1}{2}\frac{\partial^2 E}{\partial N^2}\Delta N^2 \qquad (2)$$

where $\Delta N = N - N_0$. By definition, the chemical potential of the electron cloud is the first derivative term, $\mu = (\partial E/\partial N)$, and its chemical hardness is the second derivative, $\eta = (\partial^2 E/\partial N^2)$. We note that μ is the negative of the electronegativity introduced by Mulliken. By contrast with the case of isolated species, the energy of an entity involved in a chemical bond must also be a function of the external potential generated by the presence of other species.

Second, the equilibrium state describing the chemical bond formed by two species is obtained (at constant pressure and temperature) when the chemical potentials of the two atoms involved become equal.

This approach can be applied to calculate the cation−oxide bonding energy that is schematized by the following pseudo-chemical reaction

$$\text{framework}^{\delta-}\cdots C^{\delta+} \Leftrightarrow \text{framework}^{\delta'-} + C^{\delta'+}_{\text{mobile}} \quad (3)$$

where C is the alkali metal cation and framework is the solid oxide framework where the mobile cation C^{+}_{mobile} moves. This pseudo-chemical reaction can also be represented by a thermally activated dissociation[21] (Figure 2). From this representation, the energy difference between the transition and equilibrium states can then be understood as the activation energy for the creation of a mobile charge carrier corresponding to ΔE_{bond}.

Using the initial assumptions given above, quasi-chemical reactions such as eq 3 have been modeled by Parr and Pearson[22] and Mortier and al.[23] It can then be shown that the electron charge transfer δN, which is the difference of electron charge between the equilibrium and transition states, can be estimated by considering the variation of the electrons chemical potential of the considered entities, namely, $C^{\delta+}/C^{\delta'+}$ and framework$^{\delta-}$/framework$^{\delta'-}$. It is demonstrated that the variations of both the electron chemical potential and the chemical hardness yield the bonding energy ΔE_{bond}, which can be decomposed in three independent contributions: an electrostatic term ΔE_{elec}, a term of covalence ΔE_{cov}, and a term ΔE_{pol} associated with the polarizability of each species. Calculations and approximations that have been detailed elsewhere[16] lead to the following expressions

$$\Delta E_{\text{elec}} = \int_0^\infty \rho_C(r)\, \delta V_{C,\text{ext}}(r)\, dr + \int_0^\infty \rho_F(r)\, \delta V_{F,\text{ext}}(r)\, dr \quad (4)$$

$$\Delta E_{\text{cov}} = \frac{[\mu_{0,C} - \mu_{0,F}]^2}{4(\eta_C + \eta_F)} + \frac{(\mu_{0,C} - \mu_{0,F})}{2(\eta_C + \eta_F)} \int_0^\infty \left[\left(\frac{\partial \rho_C(r)}{\partial N}\right)\delta V_{F,\text{ext}}(r) - \left(\frac{\partial \rho_F(r)}{\partial N}\right)\delta V_{F,\text{ext}}(r)\right] dr + \cdots + \frac{1}{4(\eta_C + \eta_F)} \times \left(\int_0^\infty \left[\left(\frac{\partial \rho_C(r)}{\partial N}\right)\delta V_{C,\text{ext}}(r) - \left(\frac{\partial \rho_F(r)}{\partial N}\right)\delta V_{F,\text{ext}}(r)\right] dr\right)^2 \quad (5)$$

and

$$\Delta E_{\text{pol}} = \int\int \left(\frac{\partial \rho_C(r)}{\partial V_{C,\text{ext}}(r')}\right)\delta V_{C,\text{ext}}(r)\, \delta V_{C,\text{ext}}(r')\, dr\, dr' + \int\int \left(\frac{\partial \rho_F(r)}{\partial V_{F,\text{ext}}(r')}\right)\delta V_{F,\text{ext}}(r)\, \delta V_{F,\text{ext}}(r')\, dr\, dr' \quad (6)$$

In these equations, the subscripts C and F refer to the alkali metal cation and the solid oxide framework, respectively. $\rho(r)$ is the electron density and μ_0 is the standard electrons chemical potential of the isolated species.

The complete calculation of eqs 4−6 can only be achieved by time-consuming first-principles computations because the exact evaluation of all of the energy terms requires the knowledge of the $\rho(r)$, $V_{\text{ext}}(r)$, $\partial\rho(r)/\partial N$, and $\partial\rho(r)/\partial V_{\text{ext}}(r')$ functions for both the considered alkali metal cation C and oxide framework F. However, further approximations can be introduced and simplified expressions for each energy term are proposed. These expressions are given as a function of the alkali metal cations radius R_C.

The Electrostatic Term (Eq 4). First, it can be assumed that the variation of the external potential $\delta V_{F,\text{ext}}(r)$ that affects the framework is negligible. This approximation tends to consider a rigid framework that would not be influenced by the charge transfer associated with the cation displacement. Second, it seems reasonable, as in the AS model, to assume that the electrostatic term is proportional to the inverse of the cation radius. The coefficient of proportionality is related to the Madelung constant, which we can consider, for a given framework, to be independent of the nature of the alkali ions. Therefore, it follows[8] that

$$\Delta E_{\text{elec}} \propto \frac{1}{R_C + R_O} \quad (7)$$

where R_O is the radius of the O^{2-} ion with its charge of $-2e$ (R_O = 140 pm). The evolution of ΔE_{elec} (eq 7) is reported in Figure 3.

The Covalent Term (Eq 5). This term accounts for the electron transfer between the cation and the framework. It thus depends on the nature of both the extraframework cations C^+ and the oxide framework itself F^-. The values of $\mu_{0,C}$ and η_C are provided by Parr and Pearson[22] (Table 1). Some values of $\mu_{0,F}$ and η_F have already been estimated from simulation in some modeled zeolites and silicates[24] where it can be seen that they

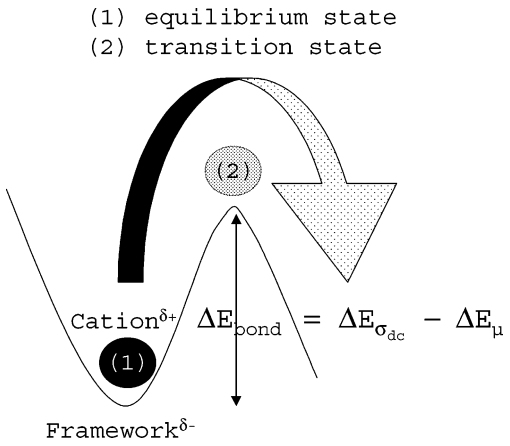

Figure 2. Schematic representation of an activated hop over a potential barrier. In our model, it is assumed that the barrier height accounts for the activation energies for both dc conductivity, $\Delta E_{\sigma_{dc}}$, and for alkali−framework bonding, ΔE_{bond}, as written in the pseudo-chemical reaction in eq 3.

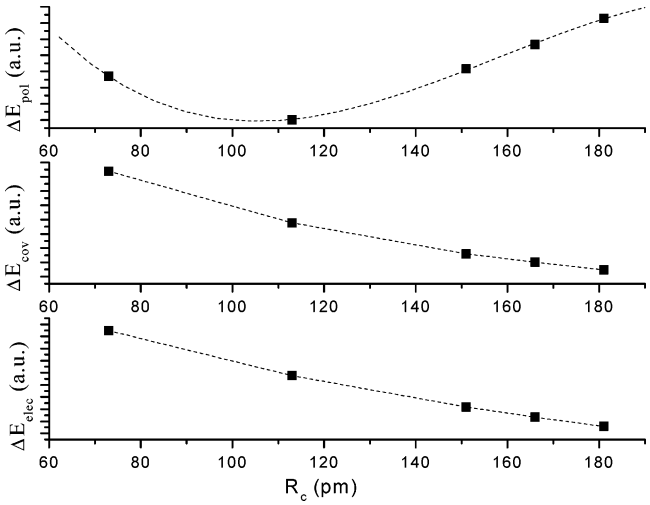

Figure 3. Evolution of the electrostatic, covalent, and polarization energy terms as a function of alkali ionic radii. Symbols represent the calculated values obtained from eqs 7, 10, and 12 and reported in Tables 2 and 3. Dashed lines are the fits corresponding to eqs 7, 11, and 14.

TABLE 1: Chemical Potential and Chemical Hardness for Each Atom and for the Various Test Cases Oxides Calculated from Eqs 8 and 9, Respectively[a]

element	$\mu_0 = -\chi_0^{22}$ (eV)	η^{22} (eV)	cation	$\mu_{0,C}^{22}$ (eV)	η_C^{22} (eV)
O	7.53	6.08	Li^+	40.5	35.1
Si	4.76	3.38	Na^+	26.2	21.1
Al	3.21	2.77	K^+	18.0	13.6
B	4.29	4.01	Rb^+	15.8	11.7
H	7.17	3.21	Cs^+	13.5	9.6
Mg	4.11	2.64			

oxide framework	chemical formula	$\mu_{0,F} = -\chi_{0,F}$ (eV)	η_F (eV)
montmorillonite	$Al_3MgSi_8O_{24}H_4$	6.32	4.68
Fau-X	$Al_{87}Si_{105}O_{384}$	6.08	4.85
Fau-Y	$Al_{64}Si_{128}O_{38}$	6.18	4.89
glassy silicate	SiO_2	6.46	5.00
glassy triborate	B_2O_3	6.01	5.15

[a] The values of $\mu_{0,F}$ and η_F used for the calculation of the covalent energy term (eq 10) have been fixed to 5 and 2 according to the theoretical calculation given in ref 24. The values reported in this table and calculated from eqs 8 and 9 are just to show that $\mu_{0,F}$ and η_F can be considered as constant in all of the test-case oxides.

TABLE 2: Calculation of the Various Preintegral Terms of Eq 5 from the Values of the Electron Chemical Potential μ_0 and the Chemical Hardness η[a]

cation	$\frac{(\mu_{0,C} - \mu_{0,F})^2}{4(\eta_C + \eta_F)}$ (eV)	$\frac{(\mu_{0,C} - \mu_{0,F})}{2(\eta_C + \eta_F)}$	$\frac{1}{4(\eta_C + \eta_F)}$ (eV^{-1})
Li^+	8.5	0.48	0.0068
Na^+	4.9	0.46	0.011
K^+	2.7	0.42	0.016
Rb^+	2.1	0.39	0.018
Cs^+	1.6	0.37	0.022

[a] Subscripts C and F refer to the alkali cation and the oxide framework, respectively. $\mu_{0,C}$ and η_C are the values reported in Table 1. $\mu_{0,F}$ and η_F are fixed to 5 and 2 eV, respectively.

vary only slightly from oxide to oxide. A rougher but faster estimation of $\mu_{0,F}$ can be obtained from the principle of electronegativity equalization proposed by Sanderson[25] and generalized by Aniya[11]

$$\mu_{0,F} = -\chi_{0,F} = -(\prod_i^N \chi_{0,i})^{1/N} \tag{8}$$

where $\chi_{0,i}$ is the electronegativity of each ith atom constituting the considered system. The chemical hardness of the oxide framework η_F can be calculated using the same approach, assuming that the ratio μ_0/η is a constant for each element[18]

$$\eta_F \propto (\prod_i^N \eta_i)^{1/N} \tag{9}$$

The values of $\mu_{0,F}$ and η_F calculated from eqs 8 and 9 are reported in Table 1. Although these values differs from those obtained by Janssen et al.[24] from computational calculations on two zeolites, i.e., a faujasite and a zeolite A, the estimation made from eqs 8 and 9 shows that $\mu_{0,F}$ and η_F can be considered as constant for all of the test-case oxides reported here. Therefore, in accordance with Janssen et al., $\mu_{0,F}$ and η_F are fixed to 5 and 2, respectively, for all of our test-case oxides. Moreover, it is clear that any small change in these parameters does not affect the main trends obtained from the model.

Once the standard chemical potential and chemical hardness are known for both the cations and the framework, it is possible to calculate the various preintegral terms of eq 5 (Table 2). The second and third terms appear to be much lower than the first one. Furthermore, knowing that the electron densities of the cation and the framework vary oppositely and that the oxide framework is considered as rigid, we assume that the integral terms in eq 5 are negligible and are likely to be the same for a given test-case oxide. We are aware of the fact that, with this assumption, we do not take into account the important role played by local fluctuations and by the framework flexibility on the nature of the chemical bond.[12] However, this assumption is the only way to simplify the expression and hence to provide an qualitative evaluation of the energy evolution for dc conductivity. ΔE_{cov} can then be simplified as follows

$$\Delta E_{cov} \propto \frac{[\mu_{0,C} - \mu_{0,F}]^2}{4(\eta_C + \eta_F)} \tag{10}$$

This energy increases when the alkali cation radius, R_C, decreases, and its evolution can be represented by a second-order polynomial function (Figure 3) for which the characteristic parameters are obtained by a nonlinear least-squares fitting procedure. The fit is represented in Figure 3 and corresponds to the following polynomial function

$$\Delta E_{cov} \approx 3.69 \times 10^{-4} R_C^{\,2} - 0.157 R_C + 17.9 \tag{11}$$

The fitting parameters are obtained for ΔE_{cov} in eV and R_C in pm. It will be shown later in this study that the contribution of ΔE_{cov} to ΔE_{bond} can be either positive or negative, depending on the variation of local environment for the alkali metal cation between its equilibrium and transition points.

The Polarization Term (Eq 6). It can be seen from eq 6 that the polarization energy is the sum of two contributions associated with the alkali metal cation and the oxide framework. As for the electrostatic and covalent terms, we assume that the framework is rigid and consequently that its contribution to the polarization energy term is negligible. In this respect, ΔE_{pol} can be reduced to the cation contribution $\Delta E_{C,pol}$ only.

The term $[\partial\rho_C(r)/\partial V_{C,ext}(r')]$ accounts for the variation of the cation electron density at point r upon a change of the external potential due to a modification of the cation environment at point r'. The exact calculation of this term is not easily achievable. However, it is thought that this problem is similar to the determination of the influence of an electrostatic potential on an electrically charged sphere. In this problem, it is known that the electron surface density plays a predominant role. The higher the surface density, the lower the influence of the external potential inside the sphere. By analogy, the influence of an external potential variation, $\delta V_{C,ext}(r')$, is more important when the external electron density of the considered cation is lower. With this simplified model,[16] $E_{C,pol}$ is assumed to be inversely proportional to a parameter, named "surface electron density" (SED), defined as

$$E_{C,pol} \propto \mathrm{SED}^{-1} = \frac{4\pi R_C^{\,2}}{N_{C,val}} \tag{12}$$

where $N_{C,val}$ is the number of valence electrons of the cation C^+. The difference in polarization energy between the transition and the equilibrium states, $\Delta E_{C,pol}$, is therefore

$$\Delta E_{C,pol} \propto \frac{4\pi(R_C^{*2} - R_C^{\,2})}{N_{C,val}} \tag{13}$$

TABLE 3: Calculation of the Inverse of the SED in pm² (Eq 12) from the Radius[32] and the Number of Valence Electrons for Each Alkali Metal Cation

cation	radius (pm)	number of valence electrons	SED^{-1} (pm^2)
Li^+	73	2	3.3×10^4
Na^+	113	8	2.0×10^4
K^+	151	8	3.6×10^4
Rb^+	166	8	4.3×10^4
Cs^+	181	8	5.1×10^4

where R_C^* is the cation radius at the saddle point. Depending on the solid oxide structure, R_C^* can be larger or smaller than R_C. Providing the oxide framework is rigid, we can assume $\Delta E_{C,pol}$ is approximated by SED^{-1} (eq 12). The inverse SED values are reported in Table 3 for each alkali cation and plotted as a function of R_C in Figure 3. It can then be seen that SED^{-1} goes through a minimum for Na^+.

As for ΔE_{cov}, we can represent ΔE_{pol} by means of a polynomial function, of third order in that case, for which the parameters are determined from a least-squares fitting procedure. The fit is reported in Figure 3 and corresponds to the following polynomial function

$$\Delta E_{pol} \propto -6.97 \times 10^{-2} R_C^3 + 32.9 R_C^2 - 4.62 \times 10^3 R_C + 2.22 \times 10^5 \quad (14)$$

The fitting parameters are obtained with SED^{-1} given in pm^2 and R_C in pm.

Signs of ΔE_{elec}, ΔE_{cov}, and ΔE_{pol}. We now discuss the sign of each energy contribution. It is clear that, in solid oxides where the ionic character of the alkali−oxide bond is predominant, the electrostatic contribution to the bonding energy is the largest one. Therefore, both ΔE_{elec} and ΔE_{bond} must have the same sign, i.e., positive. However, the contributions of ΔE_{cov} and ΔE_{pol} to ΔE_{bond} can be either positive or negative. In both cases, the sign can be related to the variation of the environment of the alkali metal cation between the transition and equilibrium states. On one hand, the cation can be more strongly confined in the equilibrium state than in the transition state. This can be the case when the transition state is located at the surface of an empty volume as for porous oxides (see Figure 4a). Then, it follows that $R_C^* > R_C$, and as a consequence, $\Delta E_{pol} > 0$ (eq 13). Likewise, it can be assumed that, in such a case, ΔE_{cov} is also positive because the covalent character of the alkali metal−oxide framework bond is likely to be higher for the equilibrium (more confined) state than for the transition state. On the other hand, stronger constraints might appear at the saddle point when, for instance, the cation has to cross a rigid doorway to hop from one site to the other (Figure 4b) as for compact oxides. Then, in contrast with the first situation, $R_C > R_C^*$, and both ΔE_{pol} (eq 13) and ΔE_{cov} must be negative. This description shows that, whatever the ionic displacement mechanism, the product $\Delta E_{pol}\Delta E_{cov}$ must necessarily be positive.

III. Fitting of the Experimental Data

It is then established that the dependence of ΔE_{bond} on R_C is given by a weighted summation over each energy term

$$\Delta E_{bond} = A_{elec}\Delta E_{elec} + A_{cov}\Delta E_{cov} + A_{pol}\Delta E_{pol} \quad (15)$$

The adjustable parameters A_i can be obtained from the fit of the experimental data with a linear combination of the functions ΔE_{elec} (eq 7), ΔE_{cov} (eq 11), and ΔE_{pol} (eq 14). These parameters correspond to the product of the weight of each contribution by the coefficient of proportionality that relates the measured energy values to their associated, simplified expressions. As the coefficients of proportionality are not known, the exact weight of each contribution cannot be determined exactly. However, it is possible to make a comparison between the values obtained from the various test-case solid oxides. In this way, we arbitrarily choose as a reference the A_i values obtained from montmorillonite samples.

Last but not least, $\Delta E_{\sigma_{dc}}$ is known for most of the investigated samples, whereas ΔE_{bond} remains unknown. Moreover, as already explained in the Introduction, both energies are equal provided that the energy for the cation migration ΔE_μ is negligible. As a consequence, the fitting of the experimental values of $\Delta E_{\sigma_{dc}}$ with eq 15 should then be possible only when $\Delta E_\mu \approx 0$. If eq 15 fails to recover the experimental data, then it can be concluded that this approximation is not appropriate.

The fitting procedure is carried out by constraining the parameter A_{elec} to positive values as the contribution of ΔE_{elec} must be necessarily positive. By contrast, A_{pol} and A_{cov} can be either positive or negative provided that their product is positive. In a first step, the nonlinear least-squares procedure is achieved for a freely adjustable set of parameters A_{elec}, A_{cov}, and A_{pol} that complies with the imposed constraints. Then, we fix to zero one or two of these parameters to check whether their contribution noticeably improves the quality of the fit. If it does not, we then consider that the parameter need not be taken into

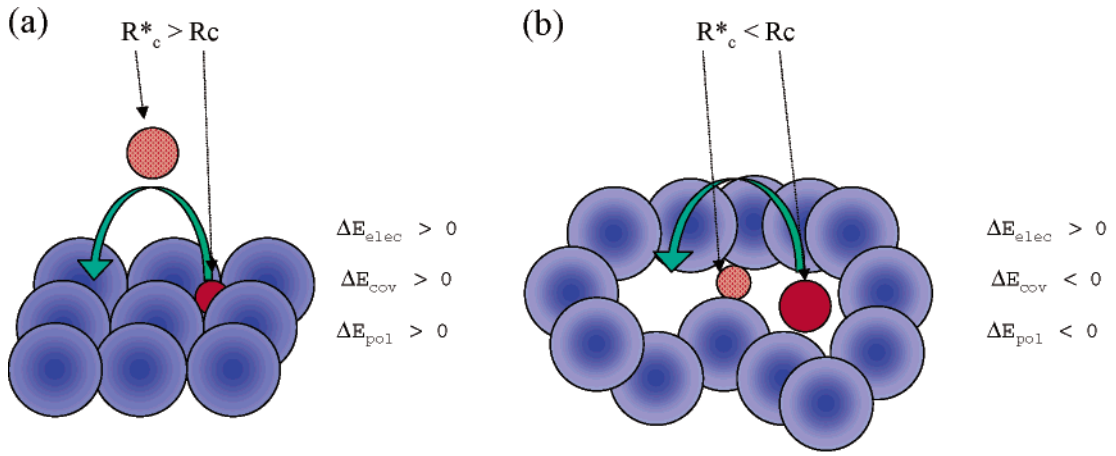

Figure 4. Schematic representations of an activated hop by which the alkali metal cation goes (a) from a more to a less confined state, i.e., in the case of porous and highly concentrated ionic glasses, and (b) oppositely from a less to a more confined state, i.e., in the case of low-concentration ionic glasses.

TABLE 4: Parameters Derived from the Nonlinear Least-Squares Fit[a] of the Experimental Data

oxide	A_{elec}	A_{cov}	A_{pol}	A^*_{elec}	A^*_{cov}	A^*_{pol}
montmorillonite	1	1	1			
Fau-Y	0.93	0	0			
Fau-X	0.28	0	2.10			
silicate glass ([C] = 1 mol·L^{-1})	0	0	5.32	1.71	−11.9	2.58
borate glass	0.61	0	2.10	1.41	−4.94	0.66
silicate glass ([C]=1.5 mol·L^{-1})	0.91	−1.4	−0.39			
borate glass (from ΔE_{bond})	1.64	−5.4	−0.55			

[a] Constraints for the fitting procedure are $A_{elec} > 0$ and $A_{cov}A_{pol} > 0$. A_{elec}, A_{cov}, and A_{pol} (see eq 15) are given with respect to the values obtained for the montmorillonite oxide taken as a reference [A_{elec}(mont) = 206 eV·pm, A_{cov}(mont) = 0.016, and A_{pol}(mont) = 0.0062 eV·pm^{-2}]. A^*_{elec}, A^*_{cov} and A^*_{pol} correspond to the results obtained when the constraints in the fitting procedure were released.

account. Finally, if this procedure does not enable us to obtain a good fit of the experimental results, then no constraints are imposed.

IV. Results and Discussion

The values of A_{elec}, A_{cov}, and A_{pol} relative to A_{i-mont} obtained for the montmorillonite sample are reported in Table 4. Recall that all of the A_{i-mont} values are positive. The experimental values of $\Delta E_{\sigma_{dc}}$ and their fits are plotted in Figure 5 when the constraints are fulfilled, i.e., for the montmorillonite and Fau-X and Fau-Y samples and the highly concentrated alkali glassy silicate. When the model fails to reproduce the experimental data, i.e., for the low-concentration silicate and for the triborate glassy oxides, we report the experimental values of $\Delta E_{\sigma_{dc}}$ and their fits both with and without constrained parameters (Figure 6). Finally, the fit of ΔE_{bond} measured on the glassy triborate[26] is reported in Figure 7.

For the sake of clarity, the results obtained on nanoporous and glassy oxides are presented and discussed separately.

Case of Nanoporous Oxides. Among the nanoporous oxides tested in this study, only the montmorillonite sample needs the three parameters A_i. The activation energy for dc conductivity of Fau-Y can be recovered by considering the electrostatic energy term only, whereas that for Fau-X also needs a significant polarization contribution. In both cases, the covalent energy can be neglected. We can now make an attempt to interpret these results in light of the oxide structure.

The structure of the dehydrated montmorillonite[27] shows that alkali cations are embedded inside the oxide layer and, hence, that the deformation of the electron cloud, i.e., the polarization, of the alkali cations becomes a nonnegligible factor for the dc conductivity activation energy. Covalent effects are more unexpected but they also can result from the confinement of alkali cations when they are embedded in their equilibrium positions into the oxide layer.

The difference between Fau-X and Fau-Y can be interpreted by focusing on both the concentrations and locations of the alkali metal cations, which are slightly different in these two zeolites.[28] The number of cations per crystallographic unit cell depends directly on the Si/Al ratio (one cationic charge per Al), which ranges from 2 to 2.5 in Fau-Y and from 1 to 1.5 in Fau-X. The higher concentration of cations in Fau-X could explain why sites I′ and II located at the center of the 6-rings of the sodalite cages and of the supercages,, respectively remain occupied, whereas sites I (in the double 6-rings between sodalite cages) are replaced

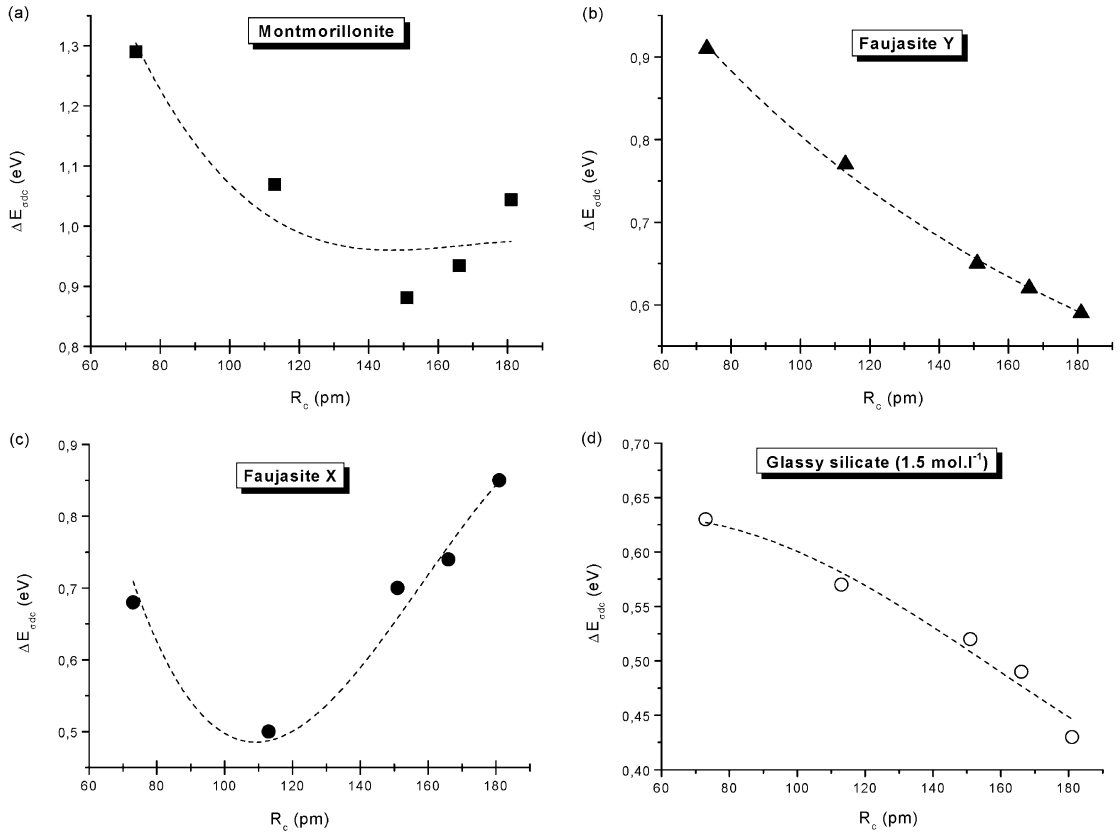

Figure 5. Constrained fits obtained with eq 15 (- - -) of the experimental (symbols) activation energy for dc conductivity for the (a) montmorillonite, (b) Fau-Y, (c) Fau-X, and (d) glassy silicate (1.5 mol·L^{-1}) samples. The corresponding parameters A_i obtained from the nonlinear least-squares fitting procedure are reported in Table 4.

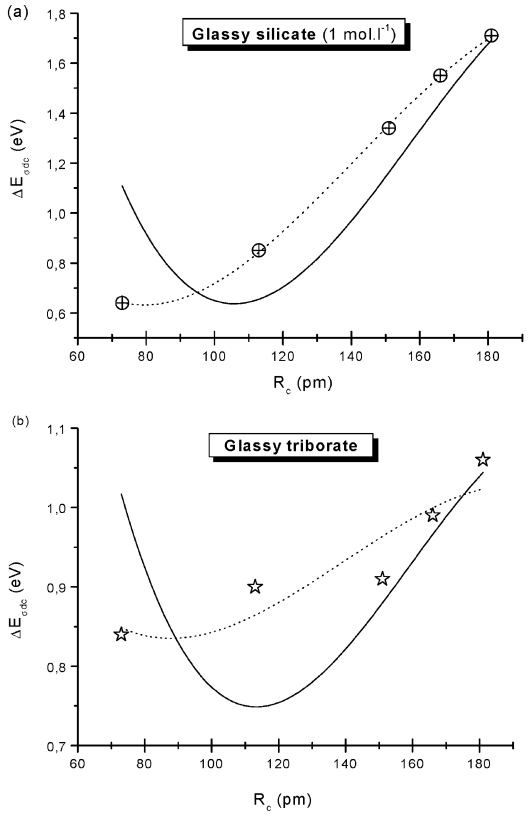

Figure 6. Constrained fits (- - -) and unconstrained fits (—) obtained with eq 15 of the experimental (symbols) activation energy for dc conductivity for the (a) glassy silicate (1 mol·L^{-1}) and (b) triborate samples. The corresponding parameters A_i (constrained fit) and A_i* (unconstrained fit) obtained by the nonlinear least-squares fitting procedure are reported in Table 4.

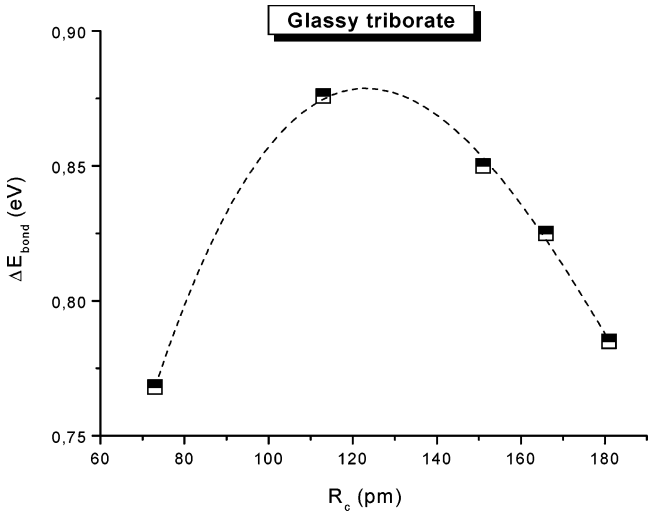

Figure 7. Constrained fits (- - -) obtained with eq 15 of the experimental bonding energy (▬)[26] for the glassy borate samples. The corresponding parameters A_i (constrained fit) obtained from the nonlinear least-squares fitting procedure are reported in Table 4.

by sites III located in 4-rings near the inner wall of the supercages. This latter site is characterized by a more confined geometry and shorter alkali metal−O and alkali metal−(Si,Al) distances than the other ones (4-rings instead of 6-rings). This could be responsible for the particular behavior of the Fau-X modeled by a larger polarization contribution than Fau-Y. The absence of covalence in both zeolites can be explained by the relatively low confined state of the alkali metal compared to their situation in montmorillonite.

Case of the Glassy Oxides. In this kind of solid oxide, the evolution of $\Delta E_{\sigma_{dc}}$ for the highly concentrated glassy silicate (Figure 5d) can be accurately described by the model. It is then emphasized that ΔE_μ can be neglected in this case. This result is in agreement with the concept of connective tissue model proposed by Ingram[14] and recently reused to explain the correlation curve observed between the structure factor Q and the average electronegativity of several superionic glasses.[13] With this concept for ionic glasses, the glassy system is considered as heterogeneous: ion-rich domains are connected to each other such that a preferred diffusion path exists throughout the structure. This structural image is, to some extent, qualitatively comparable to that of a porous network in which ions migrate without constraint once they are extracted from their equilibrium position. It is thus not surprising that an ionic glassy system having a connective tissue behaves similarly to an ionic porous oxide.

By contrast, the evolution of $\Delta E_{\sigma_{dc}}$ for the two other glassy oxides cannot be properly reproduced (Figure 6) unless both constraints are released. In that case, the fit leads to A^*_{cov} becoming negative while A^*_{pol} remains positive (see Table 4). If A^*_{cov} is maintained positive, then A^*_{elec} and A^*_{pol} become negative, and the fit is even poorer. This result clearly demonstrates that the model is not suitable for recovering the experimental behavior of $\Delta E_{\sigma_{dc}}$ in these two nonporous oxides and that the energy contribution ΔE_μ that is due to the framework deformation must be included in the model as in the AS model. Meanwhile, it is noteworthy that, in the case of these two glasses, the best constrained fit is obtained when A_{cov} and/or A_{elec} are fixed to zero (see Table 4). This trend confirms that, in addition to the contribution of the framework deformation ΔE_μ, the roles of cation polarization and, to some extent, the covalent character of the alkali metal−borate bond are relevant for explaining the evolution of $\Delta E_{\sigma_{dc}}$. Although the model is not valid for $\Delta E_{\sigma_{dc}}$, it is shown (Figure 7) that it can be successfully applied to ΔE_{bond} when the latter can be determined as in the case of the glassy triborate.[26] The fitting results are also reported in Table 4.

Comparison. The validity of the model can also be discussed by comparing the results obtained on both types of solid oxides. The main feature concerns the signs of ΔE_{cov} and ΔE_{pol}. In all nanoporous materials, the contributions of ΔE_{cov} and ΔE_{pol} are negligible or positive, whereas they are negative in all of the glassy oxides. This outcome is in accordance with the structure of these solid oxides and with the assumptions proposed in this model. In the case of the nanoporous oxides, the alkali metal cations have to be extracted from their crystallographic site located close to the surface where they are embedded, i.e., the equilibrium position, to the surface of the porosity, i.e., the transition state. Therefore, they move from a confined position to a position where the constraints are released (Figure 4a). When the alkali cation equilibrium position is just at the surface, there is no significant environment change along the displacement path. In such a case, the contributions of ΔE_{cov} and ΔE_{pol} are negligible, as in Fau-Y. When the alkali cation is more embedded in the structure, ΔE_{cov} and/or ΔE_{pol} appear to be a relevant energy term in the evolution of the activation energy for dc conductivity, i.e., in the cases of montmorillonite and, to a lesser extent, Fau-X.

On the contrary, it is often suggested that the opposite situation occurs in ionic glassy systems where ions have to move through a geometrically constrained doorway placed between

two free volumes[29]—also called "pockets"[30]—into which the alkali metal cations are more or less free to move. From our model, this description corresponds to the case depicted in Figure 4b for which ΔE_{pol} and ΔE_{bond} are negative.

V. Conclusion

Although the modeling of the experimental data proposed here can be seen as a simplistic approach to alkali cation−framework bonding in nanoporous and glassy solid oxides, it leads to interesting conclusions. First, it is well established that the various energy contributions, namely, electrostatic, covalent, and polarization can be schematized by simple functions of R_C, the radius of the considered alkali cations. Second, it is shown that the experimental data, i.e., the activation energy for dc conductivity, obtained for some nanoporous aluminosilicates can be well reproduced by a linear combination of these energy contributions. The same result is obtained for a highly concentrated ionic glassy silicate where free volumes are thought to be large enough to facilitate ionic displacement over short distances. However, the model does not fit with the experimental behaviors exhibited by the two other nonporous glassy oxides investigated in this work. In the latter, an additional energy term accounting for the framework deformation, as in the AS model, is likely to be necessary to reproduce the experimental data.

It is also pointed out that a polarization term is necessary for Fau-Y, but not for Fau-X. These different behaviors can be explained in terms of the different cation locations. This result emphasizes that classical force-field calculation including polarization effects by means of a core−shell model,[31] for instance, can be crucial for reproducing experimental data involving the alkali metal−oxide bonds. However, the covalent contribution is insignificant for both Fau-X and Fau-Y. This trend is confirmed by the successful applications of classical force-field computational simulations in this type of porous materials. Meanwhile, this behavior is not universal because the data obtained for the clay mineral studied in this work, i.e., montmorillonite, shows that a covalent energy term is needed. This result indicates that, within porous oxides, the bond formation between alkali metal cations and the oxide framework is not as easily explained as we would expect and that electron transfer between the oxide framework and the alkali metal cations is possible. This latter point depends on the environment in which the cations are trapped, provided that a higher confinement degree enhances the probability of charge transfer.

Finally, it is shown that the results obtained from our model consistently account for the microscopic mechanisms involved in the ionic displacement. A clear difference is then pointed out between the porous or "open" solid oxides and the more compact ones.

Acknowledgment. F.H. is a member of the "Institut Universitaire de France" and is deeply grateful to this institution for its financial support. It is a pleasure to thank Pr. Patrick Senet (Univ. de Dijon, France) for stimulating and fruitful discussions.

References and Notes

(1) Here, the term "structure" must be taken in a broad meaning. It can be the crystallographic or local structure; it can also account for the porosity or the heterogeneity (in the case of highly concentrated ionic glassy oxides, for instance).

(2) This is obviously not the case for "compact" crystalline solid oxides whose structures vary significantly with the alkali metal cation considered, e.g., LiCl, NaCl, etc.

(3) Haouzi, A.; Kharroubi, M.; Belarbi, H.; Devautour, S.; Henn, F.; Giuntini J. C. *Appl. Clay Sci.*, in press.

(4) Kalogeras, J. M.; Vassilikou-Dova, A. *Cryst. Res. Technol.* **1996**, *31*, 693.

(5) Kalogeras, J. M.; Vassilikou-Dova, A. *Electrical Properties of Zeolitic Catalysts. Defect and Diffusion Forum 164*. Scitec Publications: Zurich, Switzerland, 1998; p 1.

(6) Chryssikos, G. D.; Liu, L.; Varsamis, C. P.; Kamitsos, E. I. *J. Non-Cryst. Solids* **1998**, *235−237*, 761.

(7) Abe, Y.; Hosono H.; Lee, W.-H.; Kasuga, T. *Phys. Rev B* **1993**, *48*, 15621.

(8) Anderson, O. L.; Stuart, D. A. *J. Am. Ceram. Soc.* **1954**, *37*, 573.

(9) Jogad, M. S. *Mater. Lett.* **2002**, *54* (4), 249.

(10) Mattsson, M. S.; Niklasson, G. A.; Granqvist, C. G. *J. Appl. Phys.* **1997**, *81* (5), 2167.

(11) Aniya, *M. Solid State Ionics* **1995**, *79*, 259.

(12) Shimojo, F.; Aniya, M. *J. Phys. Soc. Jpn* **2003**, *72, 2702*

(13) Aniya, M.; Kawamura, J. *Solid State Ionics* **2002**, *154−155*, 343.

(14) Ingram, M. D. *Mater. Chem. Phys.* **1989**, *23*, 51.

(15) Elliott, S. R. *J. Non-Cryst. Solids* **1994**, *160*, 29.

(16) Giuntini, J. C.; Maurin, G.; Devautour, S.; Henn, F.; Zanchetta, J. V. *J. Chem. Phys.* **2000**, *113*, 4498.

(17) Mortier, W. J. *Struct. Bond.* **1987**, *66*, 125.

(18) Nalewajski, R. F. *J. Phys. Chem.* **1985**, *89*, 2831.

(19) Parr, R. G.; Yang, W. *Density Functional Theory of Atoms and Molecules*; Oxford University Press: New York. 1989.

(20) Nalewajski, R. F.; Parr, R. G. *J. Chem. Phys.* **1982**, *77*, 399.

(21) Maurin, G.; Senet, P.; Devautour, S.; Henn, F.; Giuntini J. C. *J. Chem. Phys.* **2002**, *117*, 1405.

(22) Parr, R. G.; Pearson, R. G. *J. Am. Chem. Soc.* **1983**, *105*, 7512.

(23) Mortier, W. J.; Gosh, S. K.; Shankar, S. *J. Am. Chem. Soc.* **1986**, *108*, 4315.

(24) Janssens, G. O. A.; Baekelandt, B. G.; Toufar H.; Mortier, W. J.; Schoonheydt, R. A. *J. Phys. Chem* **1995**, *99*, 3251.

(25) Sanderson, R. T. *Chemical Bonds and Bond Energy*; Academic Press: New York, 1976.

(26) Devautour, S.; Varsamis, C. P.; Henn, F.; Kamitsos, E. I.; Giuntini, J. C.; Vanderschueren, J. *J. Phys. Chem. B* **2001**, *105*, 5657.

(27) Deer, W. A.; Howie, R. A.; Zussman, J. *Rock-Forming Minerals*, 2nd ed.; Longmans: London, 1992.

(28) Olson, D. H.; *Zeolites* **1995**, 15, 439. Mortier, W. J. *Compilation of Extraframework Sites in Zeolites*; Butterworth: Guildford, U.K., 1982.

(29) Buet, F.; Giuntini, J. C.; Henn, F.; Zanchetta, J. V. *Philos. Mag. B* **1992**, *66*, 77.

(30) Sunyer, E.; Jund, Ph.; Jullien, R. *Phys. Rev. B* **2002**, *65*, Article No. 214203.

(31) Dick, B. G.; Overhauser, A. W. *Phys. Rev. B* **1958**, *112*, 90.

(32) Huheey, J. E.; Keiter, E. A.; Keiter, R. L. *Inorganic Chemistry: Principles of Structure And Reactivity*, 4th ed.; HarperCollins College Publishers: New York, 1993.